Pergamon

Tetrahedron 56 (2000) 6853–6865

TETRAHEDRON

Single-Crystal-to-Single-Crystal Enantioselective [2+2] Photodimerization of Coumarin, Thiocoumarin and Cyclohex-2-enone in the Inclusion Complexes with Chiral Host Compounds

Koichi Tanaka,[a] Eiko Mochizuki,[b] Nobuyoshi Yasui,[b] Yasushi Kai,[b] Ikuko Miyahara,[c] Ken Hirotsu[c] and Fumio Toda[d,*]

[a]*Department of Applied Chemistry, Faculty of Engineering, Ehime University Matsuyama, Ehime 790-8577, Japan*
[b]*Department of Materials Chemistry, Osaka University, Yamadaoka 2-1, Suita, Osaka 565-0871, Japan*
[c]*Department of Chemistry, Faculty of Science, Osaka City University, Sugimoto-cho, Sumiyoshi-ku, Osaka 558-8585, Japan*
[d]*Department of Chemistry, Faculty of Science, Okayama University of Science, 1-1 Ridai-cho, Okayama 700-0005, Japan*

Received 31 March 2000; accepted 8 May 2000

Abstract—Single-crystal-to-single-crystal enantioselective [2+2] photodimerization reactions of coumarin (**1a**), thiocoumarin (**1b**) and cyclohex-2-enone (**2**) were found to proceed efficiently in inclusion complexes with (*R*,*R*)-(−)-*trans*-bis(hydroxydiphenylmethyl)-2,2-dimethyl-1,3-dioxacyclopentane (**3a**), (*R*,*R*)-(−)-*trans*-2,3-bis(hydroxydiphenylmethyl)-1,4-dioxaspiro[4.4]nonane (**3b**), and (−)-1,4-bis[3-(*o*-chlorophenyl)-3-hydroxy-3-phenylprop-1-ynyl]benzene (**4**), respectively. Through these reactions, (−)-*anti*-head-to-head dimer **6a**, (+)-*anti*-head-to-head dimer **6b** and (−)-*syn-trans* dimer **10** were obtained in 100, 100 and 48% ee, respectively.

Introduction

Photodimerizations of coumarin and its derivatives have been studied extensively. However, it is still difficult to control the regio- and stereoselective [2+2]photodimerization of such enone derivatives both in solution and solid state. For example, photoirradiation of coumarin **1a** in the solid state for 48 h gives a mixture of *anti*-head-to-head dimer **6a**, *syn*-head-to-head dimer **7a** and *syn*-head-to-tail dimer **9** in only 20% yield, while photoirradiation of **1a** in water for 22 h affords **7a** in 20% yield.[1] Photodimerization of thiocoumarin **1b** in the solid state gives a complex mixture of four possible dimers, **6b**–**9b**, although (±)-**6b** is obtained when irradiated in CH_2Cl_2 solution.[2] Photoirradiation of both neat and benzene solutions of cyclohex-2-enone **2** gives a mixture of *syn-trans*-dimer **10** and *anti-trans*-dimer **11**.[3] Furthermore, the enantiocontrol of the [2+2] photodimerization reactions of coumarin, thiocoumarin and cyclohex-2-enone has not yet been reported.

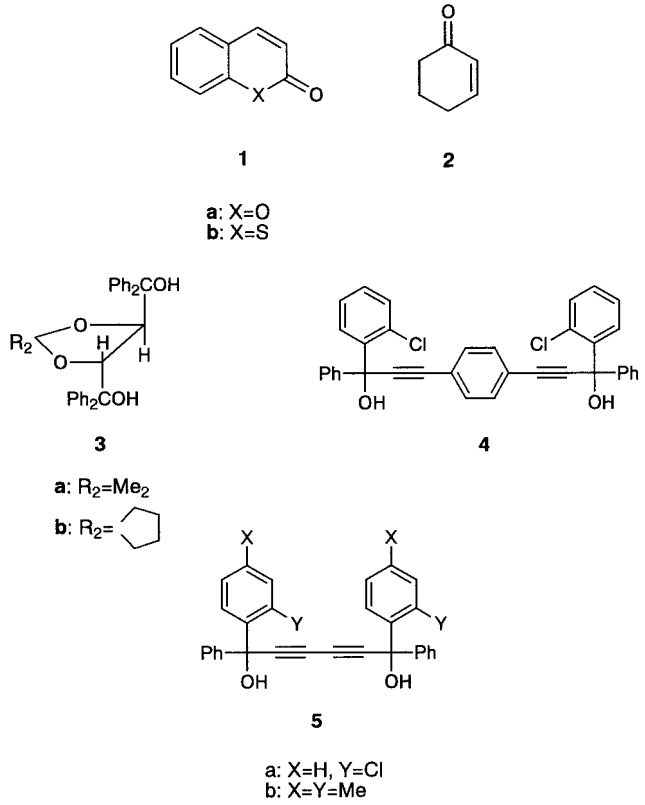

Keywords: single crystal; photodimerization; inclusion complexes.
* Corresponding author. E-mail: toda@chem.ous.ac.jp

0040–4020/00/$ - see front matter
PII: S0040-4020(00)00507-X

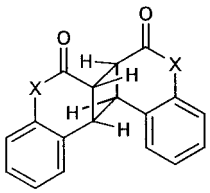

6

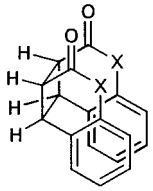

7

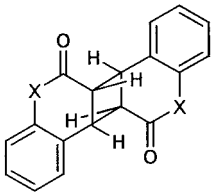

8

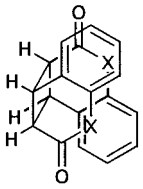

9

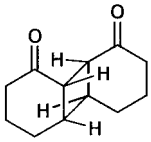

10

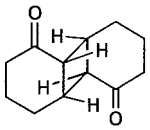

11

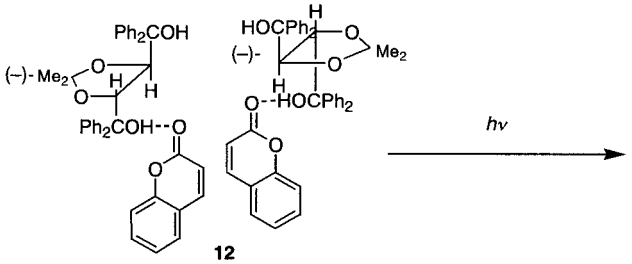

12

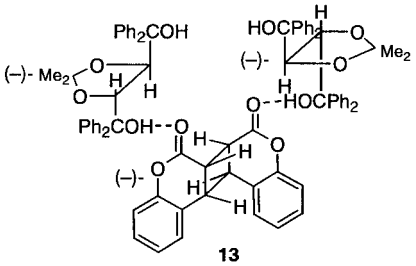

13

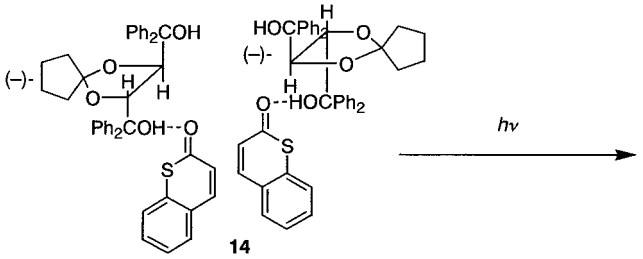

14

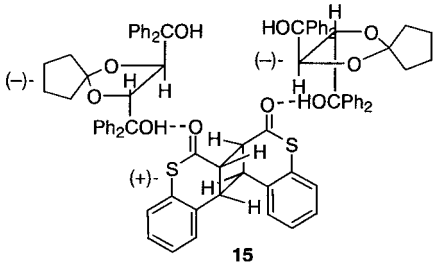

15

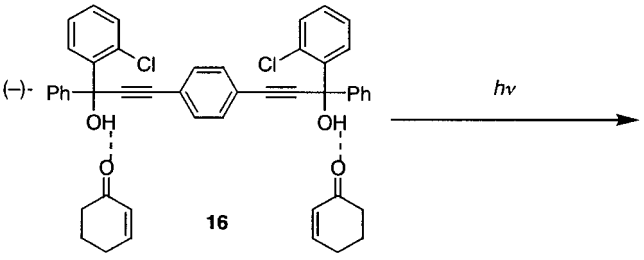

16

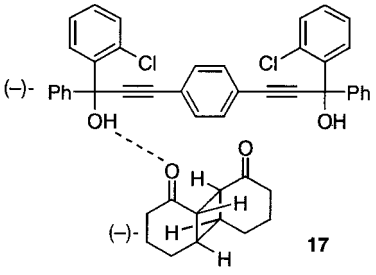

17

Recently, we have found that the stereo-, regio-, and enantio-selective photodimerization reactions of **1a**, **1b** and **2** proceed very efficiently in the inclusion complexes with various host compounds (**3**–**5**). For example, photoirradiation of the 1:1 inclusion complex **12** of (−)-**3a** with **1a** in the solid state gave optically active *anti*-head-to-head dimer (−)-**6a** in 96% yield.[4] Similar photoirradiation of the 1:2 inclusion complex of (−)-**5a** with **1a** gave *syn*-head-to-head dimer **7** in 75% yield, while racemic *anti*-head-to-tail dimer **8a** was obtained in 92% yield by photoirradiation of the 1:2 inclusion complex of *meso*-**5b** with **1a**.[4] Photoirradiation of **14**, 1:2 inclusion complex of (−)-**5a** with **1b**, and 1:2 inclusion complex of *meso*-**5b** with **1b** gave optically pure (+)-**6b**, **7b** and (±)-**8b** in 73, 74 and 69% yields, respectively.[5] Further, photoirradiation of the 1:2 inclusion complex of (−)-**4** with **2** in the solid state afforded (−)-**10** of 48% ee in 75% yield.[6]

Interestingly, we have now found that the single crystals of the inclusion complexes **12**, **14** and **16** were efficiently converted to the single crystals of the corresponding inclusion complexes **13**, **15** and **17**, respectively, upon photoirradiation in the solid state. Some examples of single-crystal-to-single-crystal photoreaction have been reported previously.[7–11] However, only a few of these involve enantioselective reactions and they are all intramolecular photocyclization reactions.[9–11] This is the first example of enantioselective intermolecular photoreaction via a single-crystal-to-single-crystal transformation in the inclusion complexes with optically active host compounds.

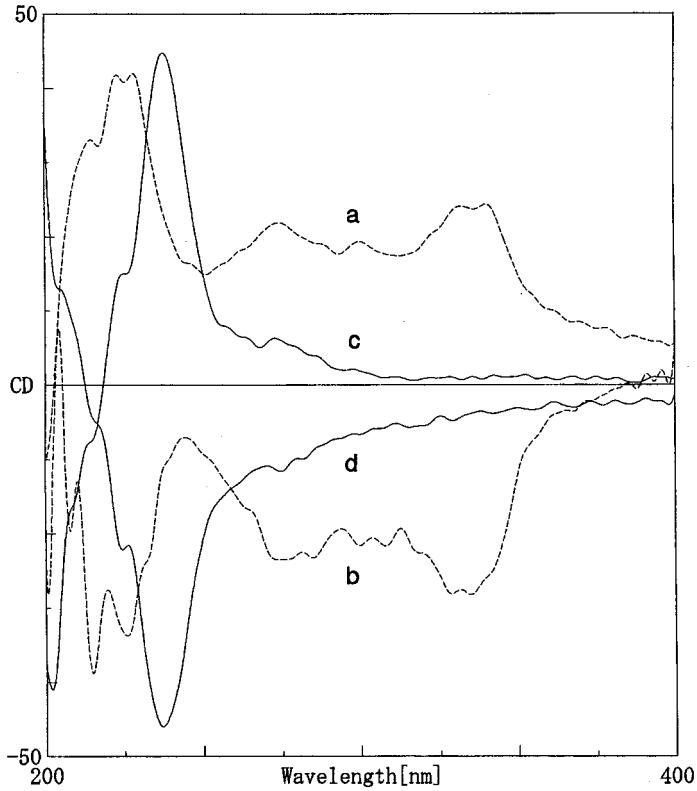

Figure 1. CD spectra in Nujol mulls: (a) a 1:1 complex of **1a** with (+)-**3a**; (b) a 1:1 complex of **1a** with (−)-**3a**; (c) a 2:1 complex of (+)-**3a** with (+)-**6a**; (d) a 2:1 complex of (−)-**3a** with (−)-**6a**.

Results and Discussion

Single-crystal-to-single-crystal enantioselective [2+2]photodimerization of coumarin 1a in the 1:1 inclusion complex with (*R*,*R*)-(−)-3a

When a solution of a 1:1 mixture of **1a** and (−)-**3a** in AcOEt–hexane was kept at room temperature for 3 h, a 1:1 inclusion complex (**12**) was obtained as colorless needles.[4] Irradiation of **12** in the solid state with a 400 W high-pressure Hg lamp (Pyrex filter, room temperature, 4 h) gave a 2:1 complex (**13**) of (−)-**3a** with (−)-**6a**. After photoirradiation, the crystals were still clear and the reaction proceeded in a single-crystal-to-single-crystal manner throughout the reaction. The (−)-*anti*-head-to-head dimer (**6a**) was isolated by replacement of the guest (**6a**) with DMF. When the 2:1 complex (**13**) was recrystallized from DMF-H_2O (5:1), a 1:1 complex of (−)-**3a** with DMF was obtained as colorless needles in 99% yield. Concentration of the filtrate left the optically pure (−)-*anti*-head-to-head dimer (**6a**) which was isolated as colorless prisms in 89% yield. The optical purity of (−)-**6a** was determined by comparison of the $[\alpha]_D$ value of enantiomerically pure **6a**.[12]

This result shows that two molecules of **1a** are arranged in chirally related position, which gives the optically active *anti*-head-to-head dimer (**6a**) by [2+2] photodimerization. This chiral arrangement of the achiral molecule **1a** in the inclusion complex (**12**) can easily be detected by CD spectral measurement of its Nujol mull. The 1:1 complex of **1a**

Table 1. Crystallographic data for a 1:1 complex (**12**) of **1a** with (−)-**2a**, a 2:1 complex (**13**) of (−)-**2a** with (−)-**3a**, a 1:1 complex (**14**) of **1b** with (−)-**2b**, a 2:1 complex (**15**) of (−)-**2b** with (+)-**3b**

Compound	(**12**) Monomer	(**13**) Dimer	(**14**) Monomer	(**15**) Dimer
Formula	$C_{40}H_{36}O_6$	$C_{40}H_{36}O_6$	$C_{42}H_{38}O_5S_1$	$C_{42}H_{38}O_5S_1$
Crystal system	Monoclinic	Monoclinic	Monoclinic	Monoclinic
Space group	*C*2	*C*2	$P2_1$	$P2_1$
a (Å)	35.59(4)	32.80(3)	10.235(2)	10.371(3)
b (Å)	9.489(4)	9.467(3)	35.78(1)	34.70(2)
c (Å)	10.03(1)	10.36(4)	9.422(2)	9.414(3)
β	102.70(4)	100.27(7)	91.00(2)	91.38(3)
V (Å^3)	3305(4)	3164(2)	3449(1)	3387(2)
Z	4	4	4	4
D_{calc}	1.23	1.29	1.26	1.28
No. of used refractions	1291	1962	4990	4178
R	0.101	0.114	0.065	0.078
Temperature (°C)	Room	Room	−50	−50

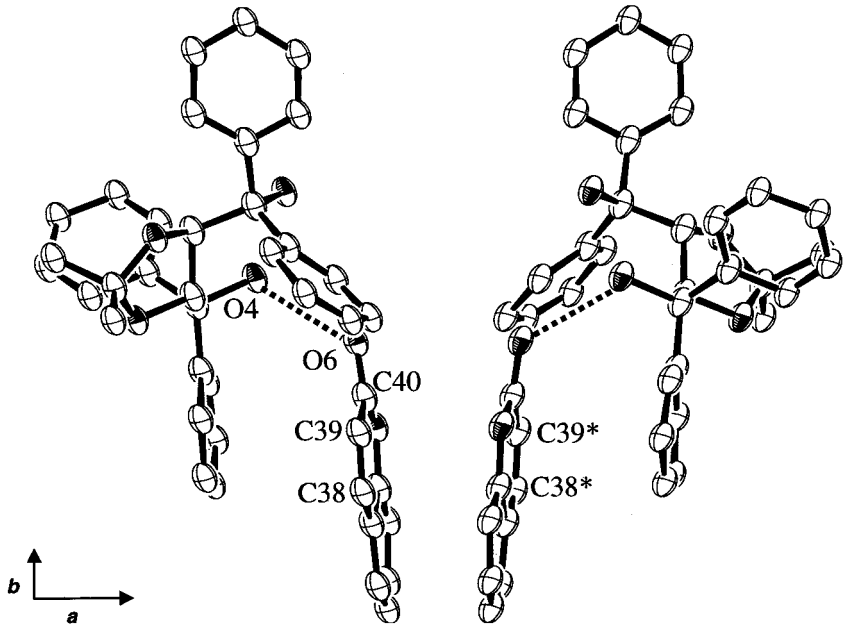

Figure 2. ORTEP drawing of the molecular structure of a 1:1 complex (**12**) of **1a** with (−)-**2a** viewed along the *a*-axis. All hydrogen atoms are omitted for clarity. The hydrogen bonding are shown by dotted lines.

with (+)- and (−)-**3a** showed CD spectra with a mirror-imaged relation (Fig. 1). After photoirradiation, the CD absorptions of **12** at 225, 275, 300 and 330 nm disappeared, and the new CD absorption due to **13** at 240 nm appeared. The photodimerization of **12** was also followed by measurement of IR spectra as Nujol mulls. Upon photoirradiation, the νCO absorption of **1a** in **12** at 1700 cm^{-1} decreased gradually and finally disappeared after 4 h, and new νCO absorption due to **6a** in **13** appeared at 1740 cm^{-1}.

The single-crystal-to-single-crystal nature and the steric course of the photodimerization of coumarin **1a** to (−)-*anti*-head-to-head dimer **3a** in the inclusion complex **12** were investigated by X-ray crystallographic analysis and X-ray powder diffraction spectroscopy. Crystal data are listed in Table 1. X-Ray crystallographic analysis showed that two molecules of **1a** were arranged by forming a hydrogen bond between the C40═O6 of **1a** and the O4–H of **3a** in the direction which gave the *anti*-head-to-head dimer (**6a**) by photodimerization and the molecular aggregation with 3.59 and 3.42 Å were short enough contact, which should react easily and topochemically.[8] After photoirradiation, the bond distances of the cyclobutane ring connecting C38–C38* and C39–C39* are 1.6 and 1.57 Å, respectively. (Figs. 2 and 3).

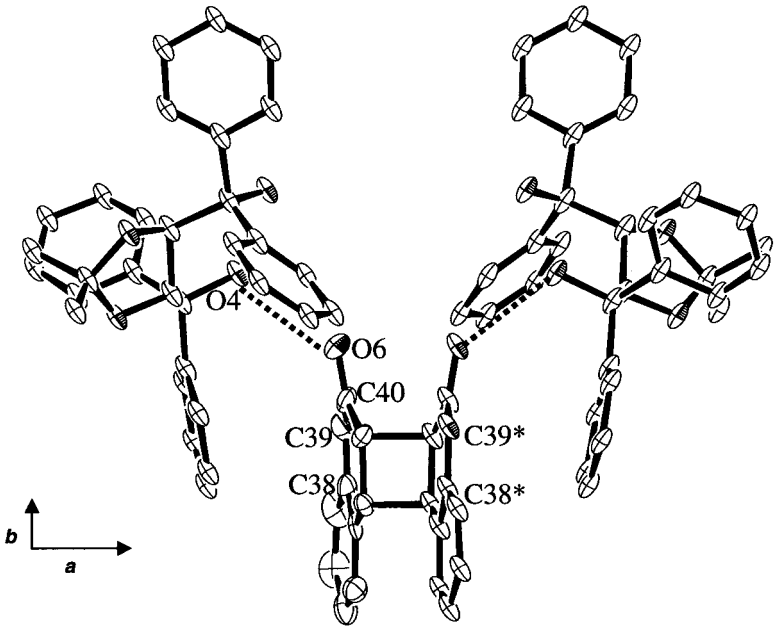

Figure 3. ORTEP drawing of the molecular structure of a 2:1 complex (**13**) of (−)-**2a** with (−)-**3a** viewed along the *a*-axis. All hydrogen atoms are omitted for clarity. The hydrogen bonding are shown by dotted lines.

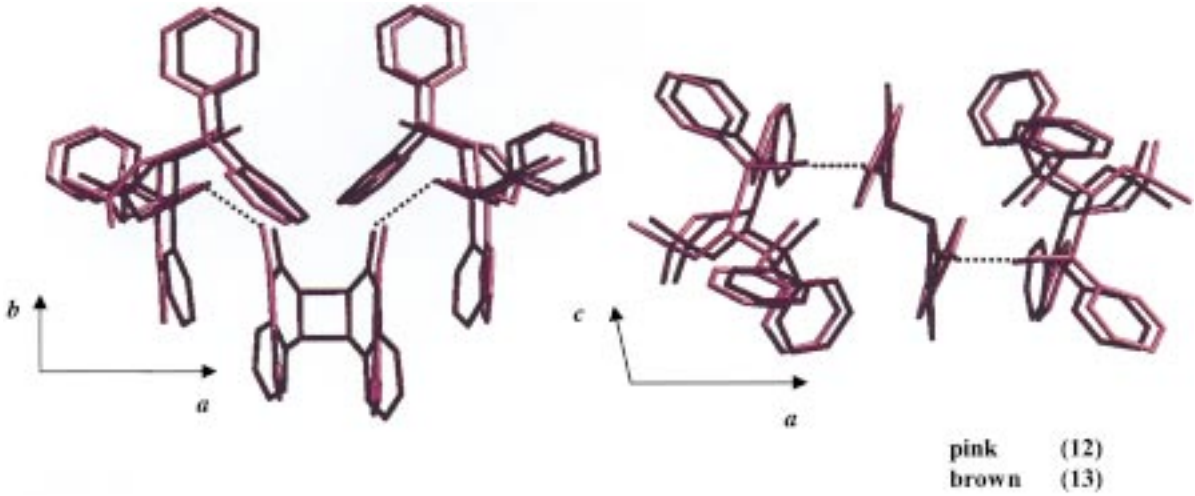

Figure 4. Superposition of monomer and dimer conformation: A 1:1 complex (**12**) of **1a** with (−)-**2a** (in pink) and a 2:1 complex (**13**) of (−)-**2a** with (−)-**3a** (in brown), left, is viewed along the *c*-axis and right is viewed along the *b*-axis. Left is viewed along the *a*-axis and right is viewed along the *c*-axis. All hydrogen atoms are omitted for clarity. The hydrogen bonding are shown by dotted lines. This drawing was prepared by the program MIDASPLUS.

The crystal-to-crystal nature of this reaction was also confirmed by X-ray powder diffraction spectroscopy. X-Ray powder diffraction patterns have been recorded by a Rigaku X-ray diffractometer RINT 2000 with a divergence slit of 1°, and an anti-scatter slit of 1° and a receiving slit of 0.15 mm. A step scan with 2θ=3–30° and a 0.02° step size, CuK_{α} radiation and a scan speed of 4°/min was used.

In the inclusion compounds **12** and **13**, the peaks at 2θ=8.90, 9.92 disappeared, and new peaks at 2θ=5.36, 8.46, 10.78 appeared during UV irradiation. After irradiation for 4 h, the original crystal structure was converted almost completely to the new structure. Remarkably, the peak of 2θ=9.92 (interplanar spacing of (400)) corresponding to a quarter of the length of *a*-axis shifted to 2θ=10.78. The latter peak corresponds to the interplanar spacing of (400) for the 2:1 complex **13** (Fig. 5).

The difference between molecular structures and crystal structures of **12**–**13** were shown in Figs. 4 and 6, respectively. As seen in Fig. 3, the cyclobutane ring forms approximately along the *a*-axis. This corresponds well to the anisotropic changes in the lattice constants.

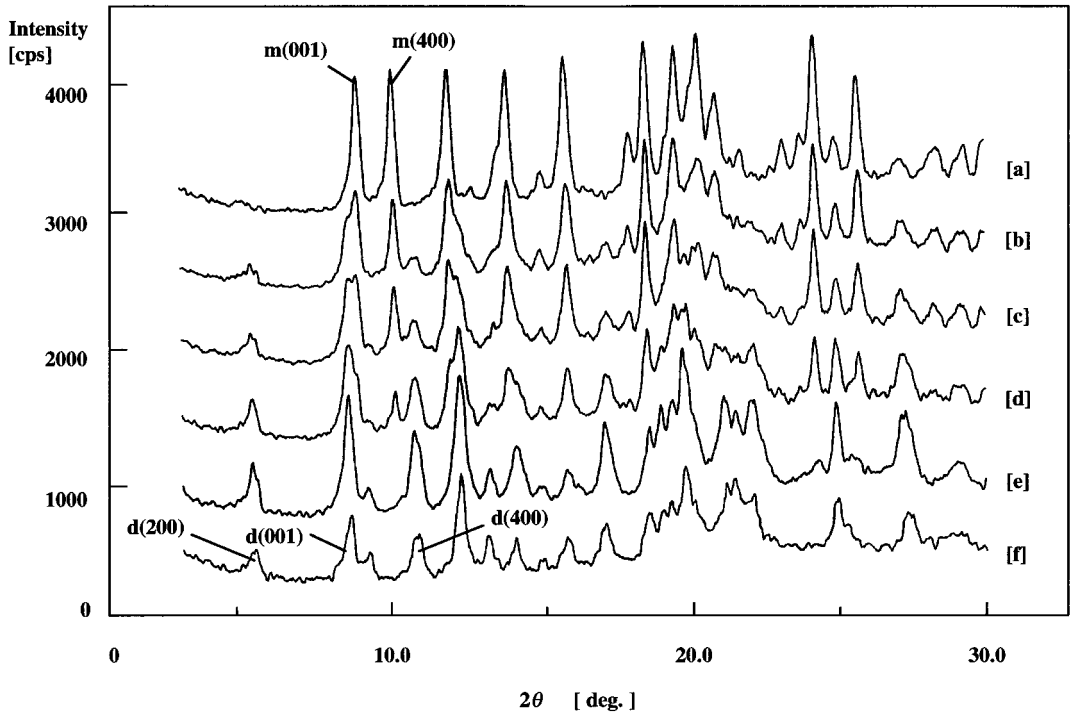

Figure 5. X-ray powder diffraction patterns of: (a) a 1:1 complex (**12**) of **1a** with (−)-**2a**; (b) after UV irradiation for 10 min; (c) after UV irradiation for 30 min; (d) after UV irradiation for 90 min; (e) after UV irradiation for 4 h; (f) a 2:1 complex (**13**) of (−)-**2a** with (−)-**3a**. m(001) and m(400) in [a] are the mirror indices for complex (**12**). d(200), d(001) and d(400) in [f] are the mirror indices for complex (**13**).

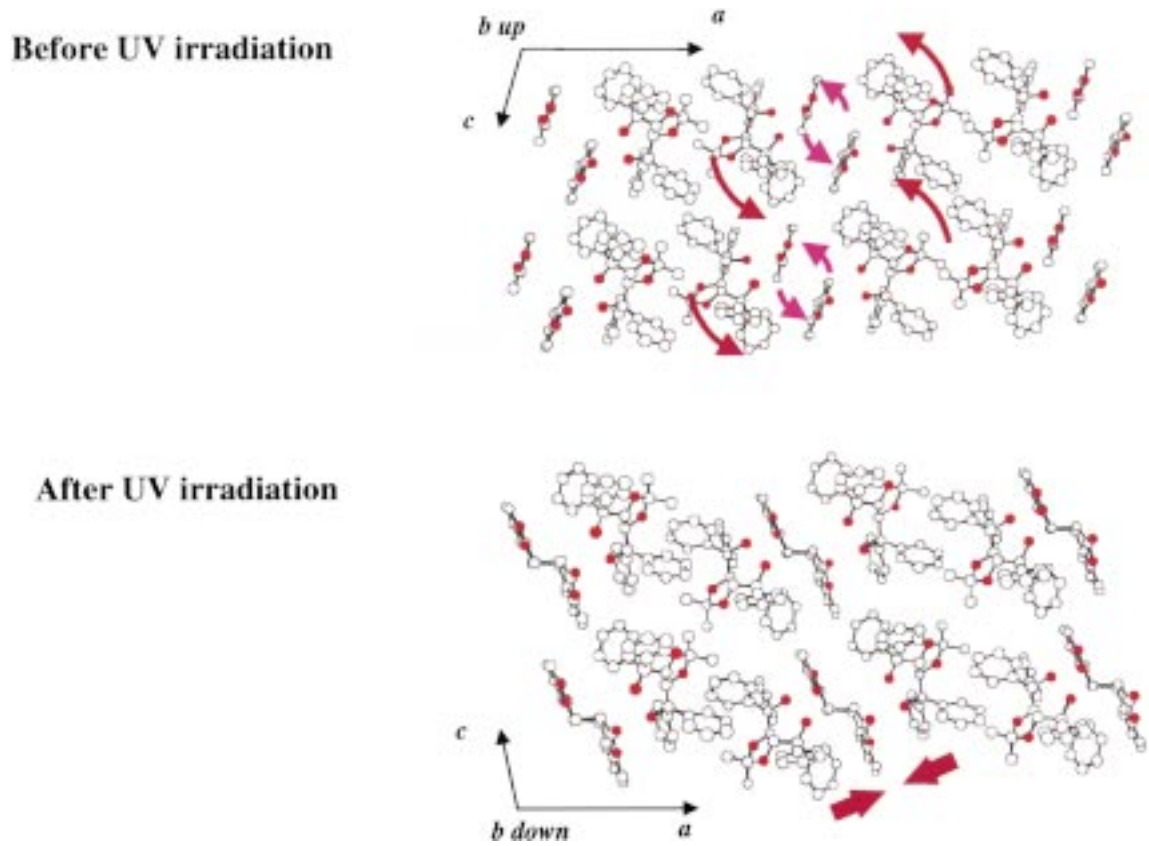

Figure 6. Comparison of the crystal structures for complex (**4**) and (**5**) before and after UV irradiation. For clarity, hydrogen atoms are not shown.

On the host molecule, it is revealed in Fig. 4 that there is not so much movement, though molecular structure of the coumarin moiety is changed largely with the formation of cyclobutane ring. The creation of C–C bond to cyclobutane effcts a slight change in the cell dimensions, but leads to the reduction of the C–C distance (ca. 1.9 Å) in **13** (1.6 and 1.57 Å) as compared to that of the starting **12**.

It is revealed that the one of phenyl groups of host molecule of **12** and **13** have a contact to coumarin ring through $\pi-\pi$ interactions. The coumarin ring moves toward in direction from *ac*-axis to *a*-axis vertically with the formation of cyclobutane after photoirradiation (pink (**12**) and brown (**13**) in Fig. 4 (right)).

In the crystal structure of **12** and **13**, these molecular arrangement greatly changes, and the whole transfer is occurred along the *ac*-axis, and the lattice constant is not almost different from −0.02 Å in *b*-axis through the reaction, and the change of lattice constant is 2.45 and +0.35 Å in *a*- and *c*-axis, respectively. Through the reaction, the change of the *ac*-axis is related to the value of β in the crystal structure. The description of causing large change of β, that is −2.43°, is explicable, in the reaction (Fig. 6).

Single-crystal-to-single-crystal enantioselective [2+2]photodimerization of thiocoumarin 1b in the 1:1 inclusion complex with (*R*,*R*)-(−)-3b

The enantioselective photodimerization of thiocoumarin (**1b**) to optically pure (+)-*anti*-head-to-head dimer (**6b**) in the 1:1 inclusion complex (**14**) of **1b** with (−)-**3b** was also found to proceed in a single-crystal-to-single-crystal manner. For example, when a mixture of thiocoumarin **1b** and optically active host compound (*R*,*R*)-(−)-**3b** in butyl ether was kept at room temperature for 12 h, a 1:1 inclusion complex **14** of **1b** with (−)-**3b** was obtained as colorless needles.[5] Photoirradiation of **14** in the solid state (400 W high-pressure Hg lamp, Pyrex filter, room temperature, 2 h) gave a 2:1 complex (**15**) of (−)-**3b** with (+)-**6b**, quantitatively; (+)-**6b** of 100% ee was isolated in 73% yield by column chromatographic separation. The crystal-to-crystal nature of this reaction was also confirmed by X-ray powder diffraction spectroscopy.

Chiral transformation of the achiral molecule **1b** in the inclusion complex (**14**) can easily be detected by CD spectral measurement of its Nujol mull. The 1:1 complex of **1a** with (+)- and (−)-**3b** showed CD spectra with a mirror-imaged relation (Fig. 7). After photoirradiation, the CD absorptions of **14** at 260 and 320 nm disappeared, and the new CD absorption due to **15** at 270 and 330 nm appeared.

The single-crystal-to-single-crystal nature and the steric course of the photodimerization of thiocoumarin **1b** to (+)-*anti*-head-to-head dimer **6a** in the inclusion complex **14** were investigated by X-ray crystallographic analysis and X-ray powder diffraction spectroscopy. Two molecules of **1b** in a 1:1 inclusion complex **14** of **1b** with (−)-**3b** are related to a pseudo two-fold axis along *c*-axis (Fig. 8). C75═O9, C84═O10 of **1b** and the O4–H, O7–H of **3b** form a hydrogen bond in the direction which gives the

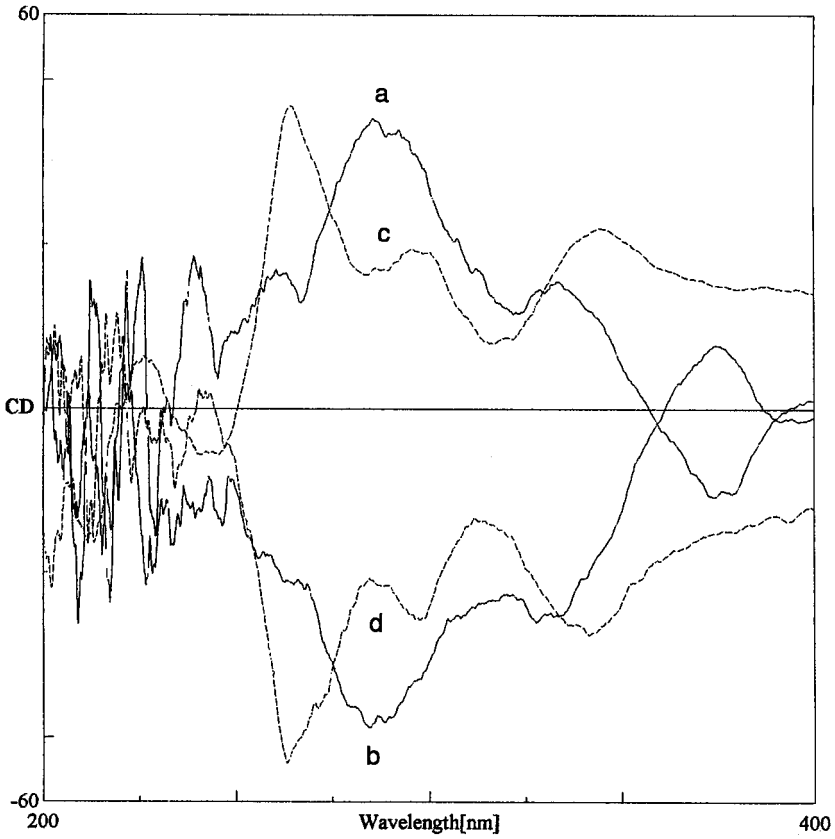

Figure 7. CD spectra in Nujol mulls: (a) a 1:1 complex of **1b** with (+)-**3a**; (b) a 1:1 complex of **1b** with (−)-**3a**; (c) a 2:1 complex of (+)-**3a** with (−)-**6b**; (d) a 2:1 complex of (−)-**3a** with (+)-**6b**.

anti-head-to-head dimer (**6b**) (Fig. 9). The distance between the two ethylenic double bonds is short enough (3.73 and 3.41 Å) to react easily and topochemically.[8] After photo-irradiation, the bond distances of the cyclobutane ring connecting C74–C83 and C73–C82 are 1.60 and 1.60 Å, respectively. The distance of atoms formed hydrogen bond are (O4–H···O9=C75, O7–H···O10=C84) are 2.81 and 2.77 Å in a 1:1 inclusion complex **14** of **1b** with (−)-**2b**,

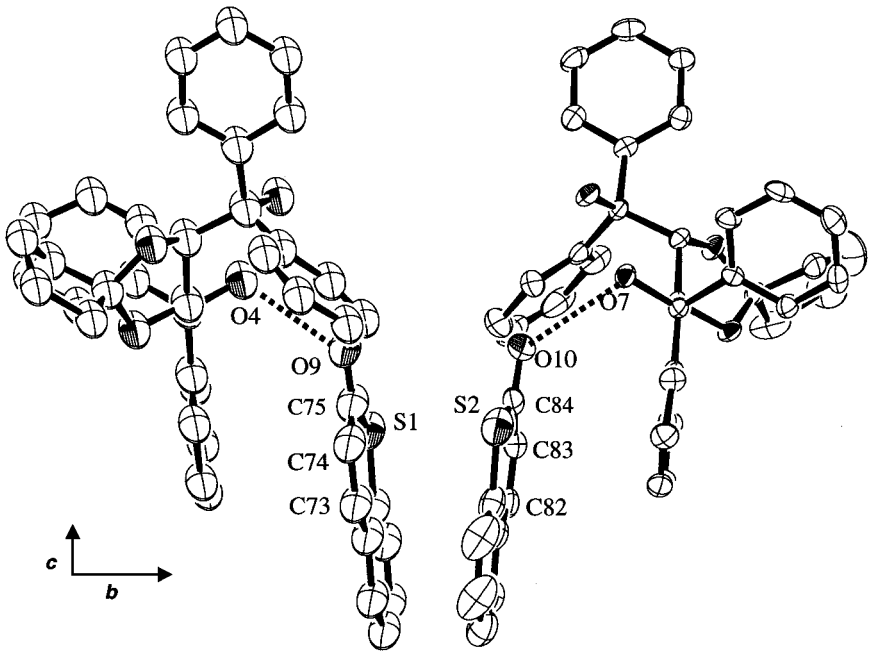

Figure 8. ORTEP drawing of the molecular structure of a 1:1 complex (**14**) of **1b** with (+)-**2b** viewed along the *a*-axis. All hydrogen atoms are omitted for clarity. The hydrogen bonding are shown by dotted lines.

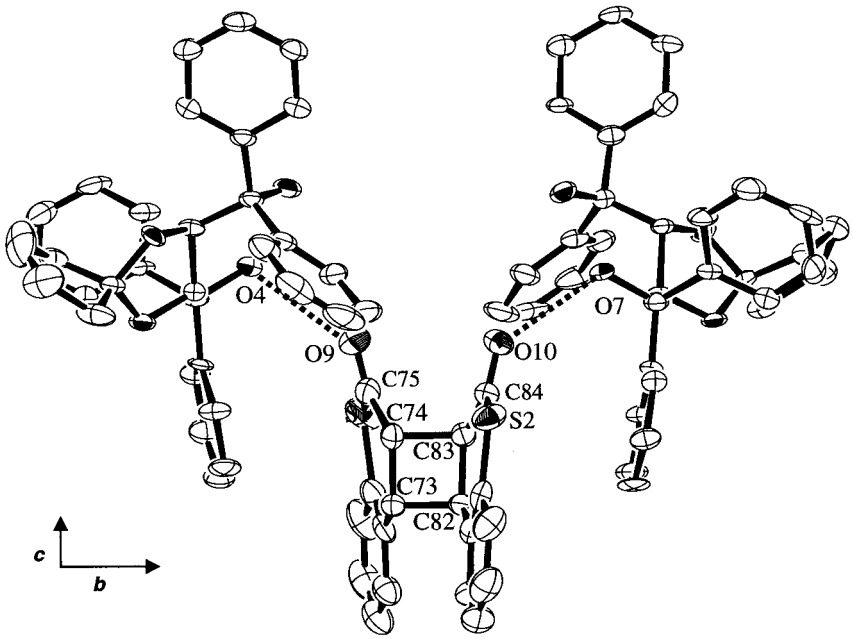

Figure 9. ORTEP drawing of the molecular structure of a 2:1 complex (**15**) of (−)-**2b** with (+)-**3b** viewed along the *a*-axis. All hydrogen atoms are omitted for clarity. The hydrogen bonding are shown by dotted lines.

respectively. In a 2:1 complex **15** of (−)-**2b** with (+)-**3b**, these corresponding distances are 2.92 and 2.85 Å. These distances can cause hydrogen bonding, while the distances after photoirradiation are rather longer than those before irradiation.

In the inclusion compounds **14**, **15**, the peaks at 2θ=8.64, 9.42 disappeared, and new peaks at 2θ=5.20, 8.76, 10.32 appeared during UV irradiation. After irradiation for 4 h, the original crystal structure had been transformed almost completely to the new structure. The peak corresponding to a quarter of the length of *b*-axis (interplanar spacing of (040)) had shifted from 2θ=9.42 to 2θ=10.32. The latter peak is equal to the interplanar spacing of (040) for the 2:1 complex **15** (Fig. 10). From these data, we conclude that the photodimerization of the 1:1 complex **14** proceeded in a single-crystal-to-single-crystal manner.

During the conversion of **14** to **15**, a similar conformational change was observed in a single crystal. From the superposition of molecular structure, thiocoumarin ring and phenyl group are stacked to synchronous transform in the case of **12** to **13**, and little rotation occurs in crystal state.

In the crystal structure, the changes in lattice constants from **14** to **15** were −0.136 and −0.008 Å for *a* and *c*, respectively, and were almost equal after the photoirradiaton. The length of *b*-axis, however, decreased 1.08 Å with creation of cyclobutane. The molecular arrangement from **14** to **15** changed less than from **12** to **13**. The direction of their

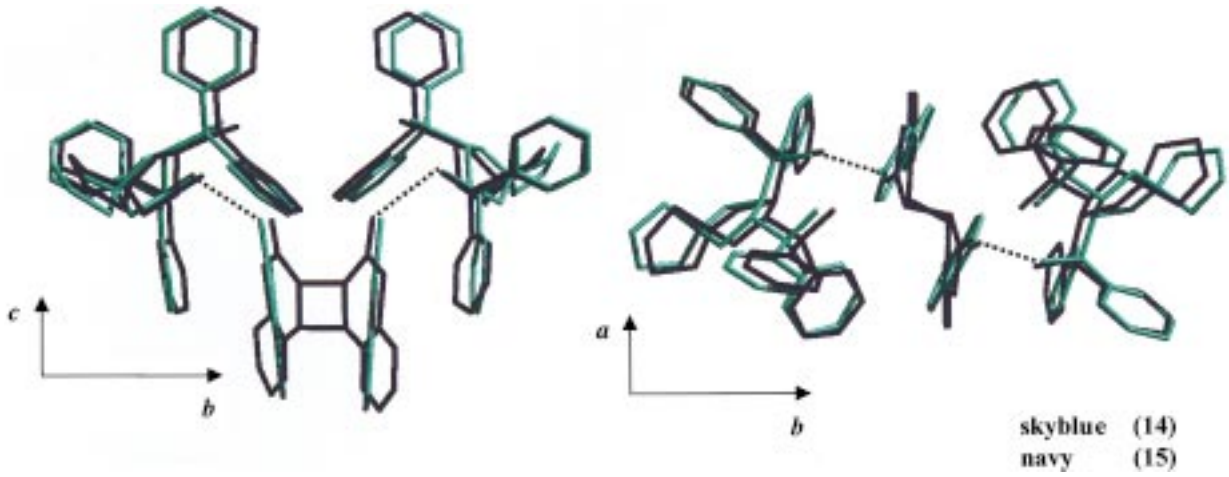

Figure 10. Superposition of monomer and dimer conformation: A 1:1 complex (**14**) of **1b** with (−)-**2b** (in skyblue), a 2:1 complex (**15**) of (−)-**2b** with (+)-**3b** (in navy), left is viewed along the *a*-axis and right is viewed along the *c*-axis. All hydrogen atoms are omitted for clarity. The hydrogen bonding are shown by dotted lines. This drawing was prepared by the program MIDASPLUS.

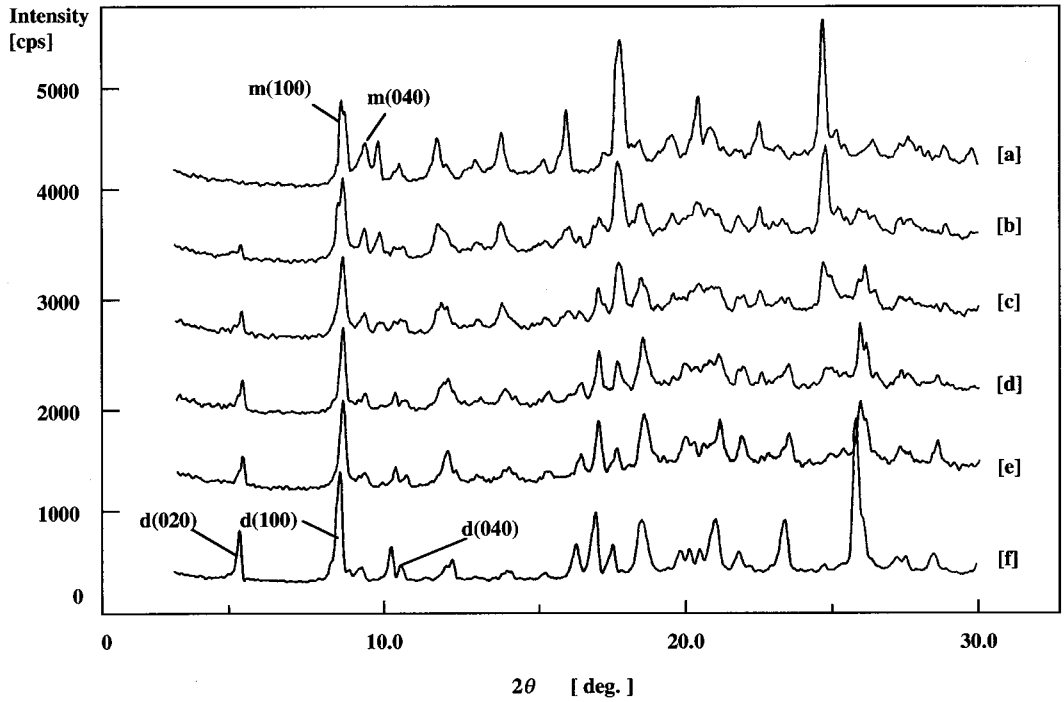

Figure 11. X-ray powder diffraction patterns of: (a) a 1:1 complex (**14**) of (−)-**1b** with (+)-**3b**; (b) after UV irradiation for 20 min; (c) after UV irradiation for 20 min; (d) after UV irradiation for 20 min; (e) a 2:1 complex (**15**) of (−)-**2b** with (+)-**3b**. m(100) and m(040) in [a] are the mirror indices for complex (**14**). d(020), d(100) and d(040)in [f] are the mirror indices for complex (**15**).

rotation is almost parallel in *b*-axis, and the change of β angle is also small with +0.38° (Fig. 11).

This situation corresponds well to the anisotropic alteration in the lattice constant. The degree of change in the crystal structure also influences photodimerization reaction rate in the solid state. Their molecular rearrangement corresponds to their photoreaction rate (see Fig. 12).

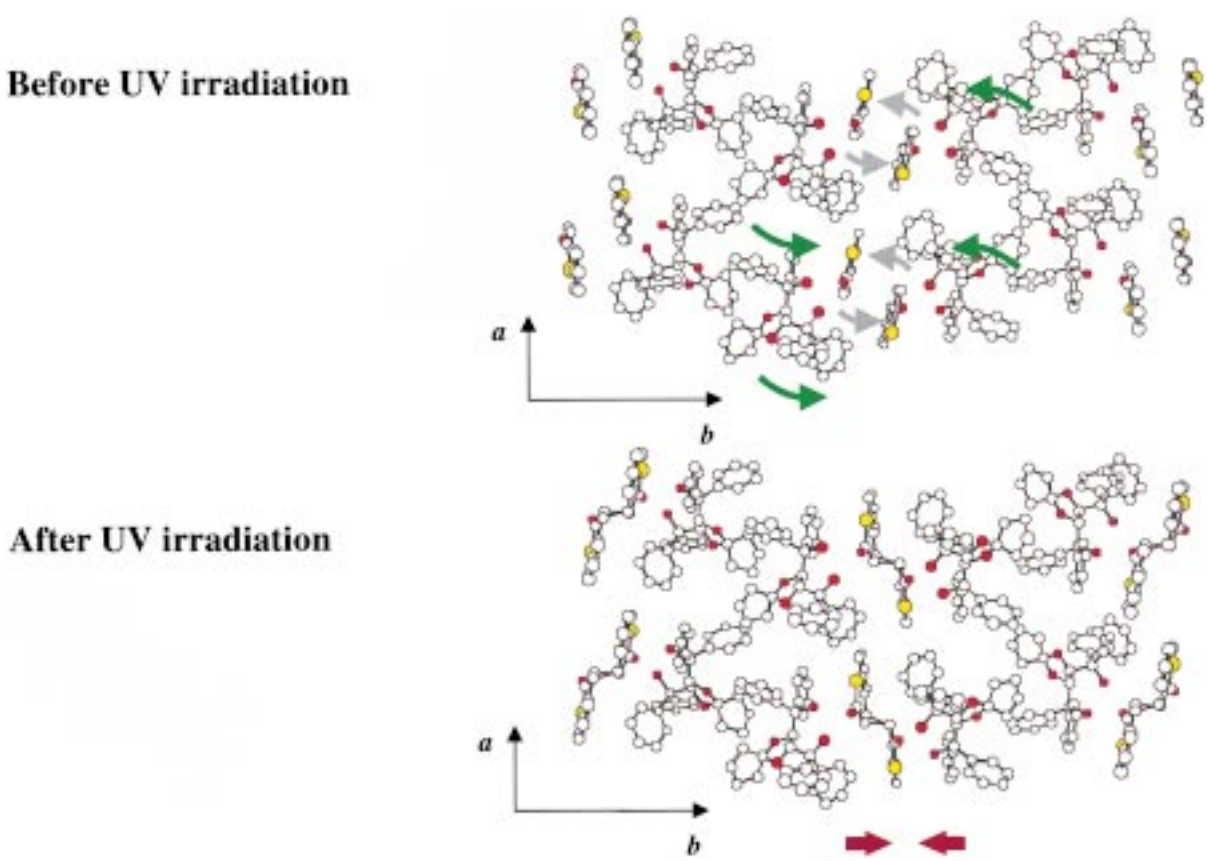

Figure 12. Comparison of the crystal structures for complex (**14**) and (**15**) before and after UV irradiation. For clarity, hydrogen atoms are not shown.

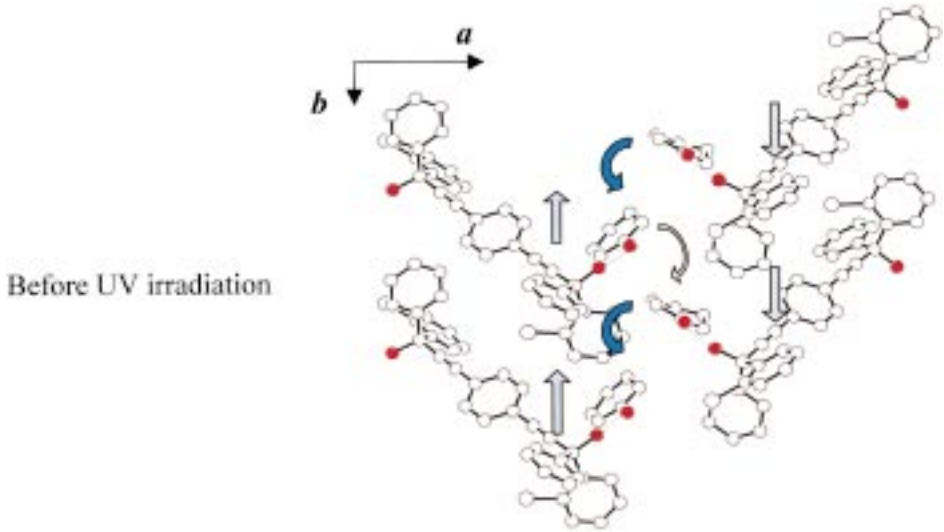

Figure 13. Molecular packing and hydrogen bonding of the complex crystal **16** viewed down the *c*-axis. The hydrogen bonds are shown by thin lines.

Single-crystal-to-single-crystal enantioselective [2+2] photodimerization of cyclohex-2-enone in the inclusion crystals with (−)-1,4-bis[3-(*o*-chlorophenyl)-3-hydroxy-3-phenylprop-1-ynyl]benzene

A solution of (−)-**4** and **2** in ether–hexane (1:1) was kept at room temperature for 6 h to give a 1:2 complex (**16**) of (−)-**4** and **2** as colorless prisms in 91% yield.[6] Photoirradiation of single-crystals of **16** (mp 90–95°C) with 400 W high-pressure Hg-lamp through Pyrex filter for 24 h gave single-crystals of a 2:1 complex **17** (mp 79–84°C) of **4** with (−)-**10**, which upon distillation in vacuo to give (−)-**10** of 46% ee in 75% yield.[6] When the reaction was carried out at −78°C in the solid state for 30 h, (−)-**10** of 58% ee was obtained in 55% yield. After photoirradiation, the crystal was still clear and the reaction proceeded in a single-crystal-to-single-crystal manner throughout the reaction.

The photodimerization reaction of **2** in **16** was followed by solid-state IR spectra as Nujol mulls. The νC=O absorption of **2** in **16** at 1660 cm^{-1} decreased gradually and finally disappeared after 24 h, and new νC=O absorption due to **10** in **17** appeared at 1695 cm^{-1} as the reaction proceeded. The single-crystal-to-single-crystal nature of the reaction was confirmed by X-ray single crystal structure analysis. The host molecules **4** in the complex crystal **16** stack along the *a*-axis, to make the inclusion columns, where the guest molecules **2A** and **2B** are alternately located (Fig. 13). The arrangement of the host molecules in the complex crystal **17** (Fig. 14) was similar to that of the complex crystal **16** (Fig. 13). But the host molecules in the complex **17** (Fig. 14) shifted about 0.73 Å along the *a*-axis, compared with the hosts in the complex (Fig. 13) with a slight decrease in the unit cell volume by 29.4 $Å^3$. The guest molecule (photoreaction product) could be located as (−)-**10** in the inclusion column with the considerably distorted shape from the ideal one and the large apparent thermal motion perpendicular to the molecular plane. However, there should be (+)-**2** as a minor product in the complex crystal **17**, since the reaction product consists of (−)-**2** and (+)-**2** in about 3:1 ratio.

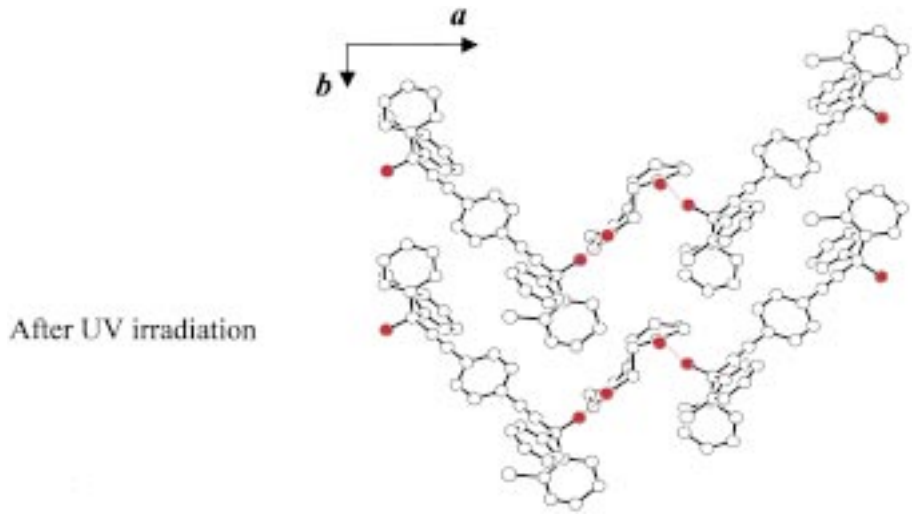

Figure 14. Molecular packing and hydrogen bonding of the complex crystal **17** viewed down the *c*-axis. The hydrogen bonds are shown by thin lines.

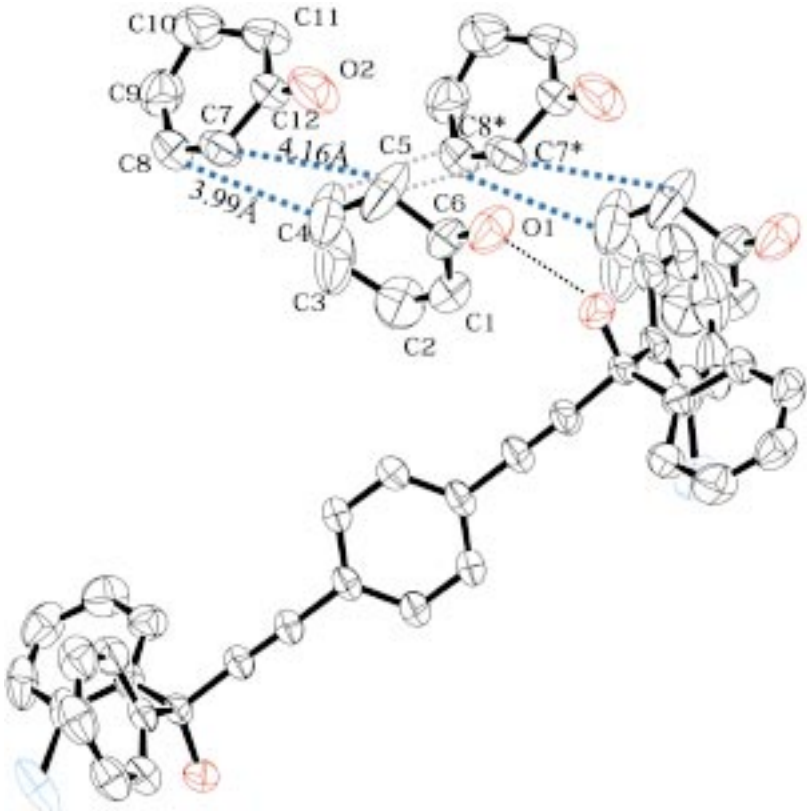

Figure 15. A view of the arrangement of the guest and the host molecules in the complex crystal **16**. **2B*** is obtained by the unit translation of **2B** along the *a*-axis, respectively. The contacts of the C4–C5 bond with the C7–C8 and C7*–C8* bonds are shown by dotted lines.

Fig. 15 shows the arrangement of the guests (**2A**, **2B** and **2B***) and the host in the complex **16**. The C4–C5 bond in **2A** makes a short contact with the C7–C8 in **2B** (C4–C8=3.99, C5–C7=4.16 Å) giving the reaction product of (−)-**2**. The distances between the π orbital lobe apexes are 1.76 Å for C4 and C8, and 1.56 Å for C5 and C7 atoms.[13] The π orbital apex is chosen as that point the π orbital axis that intersects the van der Waals surface of the atom. Another factor to help the reaction to proceed is the possible movement of the host molecules along the *a*-axis through the photodimerization reaction. The comparison of the crystal structure of **16** with that of **17** shows that hosts **4A** and **4B** can move parallel to the *a*-axis, but in the reverse direction, giving the close approach (about 1.4 Å) of **2A** and **2B**, which are hydrogen bonded to **4A** and **4B**, respectively. The mirror image ((+)-**2**) of the major product will be given if the molecule **2A** rotates toward **2B*** along the axis joining C3 and C6 atoms, and C4–C5 bond of **2A** approaches to react with C7*–C8*. The long distances between C4–C5 and C7*–C8* bonds (C4–C8*=4.82 and C5–C7*=4.46 Å) makes this approach difficult, resulting in the formation of (+)-**2** as a minor product.

Experimental

IR spectra were recorded on a JASCO FT-IR 300 spectrometer, and NMR spectra were measured on a JEOL Lambda-300 spectrometer. Optical rotations were measured on a JASCO DIP-1000 polarimeter.

Photodimerization of coumarin 1a in the inclusion complex 12. When a solution of **1a** (10.0 g, 21.5 mmol) and (−)-**3a** (3.2 g, 21.9 mmol) in AcOEt (20 ml)-hexane (100 ml) was kept at room temperature for 3 h, a 1:1 inclusion complex (**12**) was obtained as colorless needles (5.7 g, 43%, mp 95–98°C).[6] IR (Nujol): νC=O: 1700 cm^{-1}, νC=C: 1607 cm^{-1}, νOH: 3358, 3230 cm^{-1}. Elemental analysis calcd for $C_{40}H_{36}O_6$: C 71.37, H 3.99; found: C 71.64, H 3.82. Photoirradiation of **12** (1.0 g, 1.6 mmol) was carried out in the solid state by using 400 W high-pressure Hg-lamp through Pyrex filter at room temperature for 4 h. This reaction gave a 2:1 complex (**13**) of (−)-**3a** with (−)-**6a**, quantitatively. Colorless needles. Mp 228–232°C. IR (Nujol): νC=O: 1740 cm^{-1}, νOH: 3433, 3262 cm^{-1}. Elemental analysis calcd for $C_{40}H_{36}O_6$: C 71.37, H 3.99; found: C 71.64, H 3.82. When the 2:1 complex (**13**) (1.0 g) was recrystallized from DMF-H_2O (5:1, 5 ml), a 1:1 complex of (−)-**3a** with DMF was obtained as colorless prisms (0.86 g, 99%). Concentration of the filtrate left after separation of the 1:1 DMF complex with (−)-**3a**, optically pure (−)-*anti*-head-to-head dimer (**6a**) (0.17 g, mp 168–169°C, $[\alpha]_D$=−9.1° (*c* 0.19, benzene), 100% ee) was obtained as colorless prisms in 89% yield after recrystallization from ethyl acetate–hexane.

Photodimerization of thiocoumarin 1b in the inclusion complex 14. When a solution of **1b** (0.66 g, 4.1 mmol) and (−)-**3b** (2.0 g, 4.1 mmol) in *n*-butyl ether (25 ml)–hexane (5 ml) was kept at room temperature for 12 h, a 1:1 inclusion complex (**14**) was obtained as colorless needles (2.1 g, 76%, mp 106–108°C). IR (Nujol): νC=O: 1618 cm^{-1},

νC=C: 1582 cm^{-1}, νOH: 3358, 3250 cm^{-1}. Elemental analysis calcd for $C_{42}H_{38}O_5S$: C 77.04, H 5.85; found: C 77.15, H 5.79. Photoirradiation of **14** (1.0 g, 1.5 mmol) was carried out in the solid state by using 400 W high-pressure Hg-lamp through Pyrex filter at room temperature for 2 h. This reaction gave a 2:1 complex (**15**) of (−)-**3b** with (+)-**6b**, quantitatively. Colorless needles. Mp 190–194°C. IR (Nujol): νC=O: 1740 cm^{-1}, νOH: 3433, 3262 cm^{-1}. Elemental analysis calcd for $C_{42}H_{38}O_5S$: C 77.04, H 5.85; found: C 77.12, H 5.90. The 2:1 complex (**15**, 1.0 g) was dissolved in toluene (5 ml) and chromatographed on silica gel using toluene–AcOEt (4:1) to give optically pure (+)-**6b** (0.18 g, 73% yield) as colorless prisms after recrystallization from toluene. Mp 254–255°C. $[\alpha]_D$=+182° (*c* 0.02, $CHCl_3$). IR (Nujol): νC=O: 1681, 1655 cm^{-1}. Elemental analysis calcd for $C_{18}H_{12}O_2S_2$: C 66.64, H 3.73; found: C 66.38, H 3.60.

Photodimerization of cyclohex-2-enone 2 in the inclusion complex 16. A solution of (−)-**4** (5.0 g, 8.94 mmol) and **2** (1.72 g, 17.9 mmol) in ether–hexane (1:1, 10 ml) was kept at room temperature for 6 h to give a 1:2 complex **16** of (−)-**4** and **2** as colorless prisms (6.1 g, 91% yield). Mp 90–95°C. IR (Nujol): νC=O: 1660 cm^{-1}. Elemental analysis calcd for $C_{48}H_{40}O_4Cl_2$: C 76.69, H 5.36; found: C 77.01, H 5.50. Photoirradiation of **16** (2.0 g, 2.66 mmol) in the solid state by using 400 W high-pressure Hg-lamp through Pyrex filter at room temperature for 24 h gave a 1:1 complex (**17**, mp 79–84°C) of (−)-**4** with (−)-**10**, which upon distillation in vacuo gave (−)-**10** of 46% ee (0.38 g, 75% yield, $[\alpha]_D$=−58.5° (*c* 0.2, MeOH)). The optical purity was determined by HPLC containing Chiralpak AS (Daicel Chemical Co. Ltd, Himeji, Japan) as the chiral solid phase. Similar photoirradiation of powdered **16** (2.0 g, 2.66 mmol) at −78°C for 30 h gave (−)-**10** of 58% ee (0.28 g, 55% yield, $[\alpha]_D$=−73.8° (*c* 0.25, MeOH)).

Crystal data for a 1:1 complex (12) of 1a with (−)-2a. $C_{40}H_{36}O_6$, FW=612.72 space group monoclinic *C*2, *a*=35.59(4) Å, *b*=9.489(4) Å, *c*=10.03(1) Å, β=102.70(4)°, *V*=3305(4) Å^3, *Z*=4, D_{calc}=1.23 g/cm^3, crystal dimensions 1.0×0.05×0.03 mm^3, μ=0.82 cm^{-1}, *T*=293 K, *R*=0.105, R_w=0.088, and *S*=2.63 for 561 parameters and 1291 unique observed reflections with [$I>3\sigma(I)$], $\Delta\rho_{max}$=0.37*e* Å^{-3}. Data of X-ray diffraction were collected by RIGAKU RAXIS-CS imaging plate two-dimensional area detector with graphite-monochromatized MoK$_\alpha$ radiation (λ=0.71070 Å) to 2θ max of 59.5°. All the crystallographic calculations were performed by TEXSAN software package of the Molecular Structural Corporation. The crystal structures were solved by the direct methods (LODEM) and refined by the full-matrix least squares. All non-hydrogen atoms and were refined anisotropically and isotropically.

Crystal data for a 2:1 complex (13) of 1a with (−)-3a. $C_{40}H_{36}O_6$, FW=612.72 space group monoclinic *C*2, *a*=32.80(3) Å, *b*=9.467(3) Å, *c*=10.360(4) Å, β=100.27(7)°, *V*=3164(2) Å^3, *Z*=4, D_{calc}=1.29 g/cm^3, crystal dimensions 0.80×0.05×0.03 mm^3, μ=0.86 cm^{-1}, *T*=293 K, *R*=0.114, R_w=0.097, and *S*=2.86 for 560 parameters and 1939 unique observed reflections with [$I>3\sigma(I)$], $\Delta\rho_{max}$=0.46*e* Å^{-3}. Data of X-ray diffraction were collected by RIGAKU RAXIS-CS imaging plate two-dimensional area detector with graphite-monochromatized MoK$_\alpha$ radiation (λ=0.71070 Å) to 2θ max of 59.5°. All the crystallographic calculations were performed by TEXSAN software package of the Molecular Structural Corporation. The crystal structures were solved by the direct methods (LODEM) and refined by the full-matrix least squares. All non-hydrogen atoms and were refined anisotropically and isotropically.

Crystal data for a 1:1 complex (14) of 1b with (+)-2b. $C_{42}H_{38}O_5S_1$, FW=654.82, space group monoclinic $P2_1$, *a*=10.235(2) Å, *b*=35.78(1) Å, *c*=9.422(2) Å, β=91.00(2)°, *V*=3449(1) Å^3, *Z*=4, D_{calc}=1.26 g/cm^3, crystal dimensions 1.0×0.2×0.15 mm^3, μ=1.36 cm^{-1}, *T*=243 K, *R*=0.065, R_w=0.169, and Goodness of Fit(*S*)=1.07 for 865 parameters and 4954 unique observed reflections with [$I>2\sigma(I)$], $\Delta\rho_{\mu ax}$=0.42*e* Å^{-3}. Data of X-ray diffraction were collected by RIGAKU RAXIS-CS imaging plate two-dimensional area detector with graphite-monochromatized MoK$_\alpha$ radiation (λ=0.71070 Å) to 2θ max of 59.9°. All the crystallographic calculations were performed by TEXSAN software package of the Molecular Structural Corporation. The crystal structures were solved by the direct methods (sir92) and refined by SHELXL93. All non-hydrogen atoms were refined anisotropically and isotropically.

Crystal data for a 2:1 complex(15) of 1b with (+)-3b. $C_{42}H_{38}O_5S_1$, FW=654.82, space group monoclinic $P2_1$, *a*=10.371(3) Å, *b*=34.70(2) Å, *c*=9.414(3) Å, β=91.38(2)°, *V*=3387(2) Å^3, *Z*=4, D_{calc}=1.28 g/cm^3, crystal dimensions 1.0×0.2×0.15 mm^3, μ=1.42 cm^{-1}, *T*=243 K, *R*=0.078, R_w=0.218, and Goodness of Fit(*S*)=1.01 for 865 parameters and 4104 unique observed reflections with [$I>2\sigma(I)$], $\Delta\rho_{max}$=0.34*e* Å^{-3}. Data of X-ray diffraction were collected by RIGAKU RAXIS-CS imaging plate two-dimensional area detector with graphite-monochromatized MoK$_\alpha$ radiation (λ=0.71070 Å) to 2θ max of 59.7°. All the crystallographic calculations were performed by TEXSAN software package of the Molecular Structural Corporation. The crystal structures were solved by the direct methods (LODEM) and refined by SHELXL93. All non-hydrogen atoms were refined anisotropically and isotropically.

Crystal data for 16. $C_{36}H_{24}O_2Cl_2{\cdot}2C_6H_8O$, monoclinic, space group $P2_1$, MoK$_\alpha$ radiation, 2θ_{max}=55°, *a*=8.411(2) Å, *b*=28.774(3) Å, *c*=8.696(2) Å, β=105.29(2)°, *U*=2028.1(8) Å^3. D_c=1.231 g/cm^3, μ=2.03 cm^{-1}, 4775 independent intensities, 4052 observed ($I>1.00\sigma(I)$), *T*=296 K, *R*=0.048, R_w=0.061, GOF=1.72, maximum residual electron density 0.17*e* Å^{-3}.

Crystal data for 17. $C_{36}H_{24}O_2Cl_2{\cdot}2C_6H_8O$, monoclinic, space group $P2_1$, CuK$_\alpha$ radiation, *a*=8.455(3) Å, *b*=28.332(3) Å, *c*=8.704(2) Å, β=106.54(2)°, *U*=1998.7(9) Å^3, D_c=1.249 g/cm^3, μ=18.06 cm^{-1}, 2θ_{max}=124.2°, 3454 independent intensities, 2850 observed ($I>1.00\sigma(I)$), *T*=296 K, *R*=0.101, R_w=0.142, GOF=3.14, maximum residual electron density 0.39*e* Å^{-3}. The X-ray data were collected on a RIGAKU AFC7R four-circle diffractometer, using $\omega/2\theta$ scan mode. All calculations were performed with the crystallographic software package TEXSAN (Molecular Structure Corporation, 1985, 1992).

The structures were solved by direct methods[14] and subsequent Fourier recycling[15], and refined by full-matrix least-squares refinement against $|F|$, with all hydrogen atoms fixed at the calculated positions. A linear decay and empirical absorption corrections were applied.[16]

References

1. Moorthy, J. N.; Venkatesan, K.; Weiss, R. G. *J. Org. Chem.* **1992**, *57*, 3292.
2. Klaus, C. P.; Thiemann, C.; Kopf, J.; Margaretha, P. *Helv. Chim. Acta* **1995**, *78*, 1079.
3. Lam, E. Y. Y.; Valentine, D.; Hammond, G. S. *J. Am. Chem. Soc.* **1976**, *89*, 3482.
4. Tanaka, K.; Toda, F. *J. Chem. Soc., Perkin Trans. 1* **1992**, 943.
5. Tanaka, K.; Toda, F. *Mol. Cryst. Liq. Cryst.* **1998**, *313*, 179.
6. Tanaka, K.; Kakinoki, O.; Toda, F. *J. Chem. Soc., Perkin Trans. 1* **1992**, 307.
7. Enkelmann, V.; Wegner, G.; Novak, K.; Wagener, K. B. *J. Am. Chem. Soc.* **1993**, *115*, 10390–10391 (and references therein).
8. Novak, K.; Enkelmann, V.; Wegner, G.; Wagener, K. B. *Angew. Chem.* **1993**, *105*, 1678–1680; *Angew. Chem., Int. Ed. Engl.* **1993**, *32*, 1614–1617.
9. Ohashi, Y.; Sakai, Y.; Sekine, A.; Arai, Y.; Ohgo, Y.; Kamiya, N.; Iwasaki, H. *Bull. Chem. Soc. Jpn* **1995**, *68*, 2517–2525.
10. Sakamoto, M.; Takahashi, M.; Kamiya, K.; Yamaguchi, K.; Fujita, T.; Watanabe, S. *J. Am. Chem. Soc.* **1996**, *118*, 10664–10665.
11. Hosomi, H.; Ito, Y.; Ohba, S. *Acta Crystallogr. B* **1998**, *54*, 907–911.
12. Saigo, K.; Yonezawa, N.; Sekimoto, K.; Hasegawa, M.; Ueno, K.; Nakanishi, H. *Bull. Chem. Soc. Jpn* **1985**, *58*, 1000–1005.
13. Kearsley, S. K. In *Organic Solid State Chemistry*; Desiraju, G. R., Ed.; Elsevier: Amsterdam, 1987; p 69.
14. Sheldrick, G. M. In *Crystallographic Computing 3*; Sheldrick, G. M., Kruger, C., Goddard, R., Eds.; Oxford University: Oxford, 1985; pp 175–189.
15. Beurskens, P. T.; Admiraal, G.; Beurskens, G.; Bosman, W. P.; de Gelder, R.; Israel, R.; Smits, J. M. M. The DIRDIF-94 program system, Technical Report of the Crystallography Laboratory, 1994, University of Nijmegen, The Netherlands.
16. North, A. C. Y.; Philips, D. C.; Mathews, F. S. *Acta Crystallogr. A* **1968**, *24*, 351.